TITLE:
Cutaneous Wounds in Mice Lacking Tumor Necrosis Factor-stimulated Gene-6 Exhibit Delayed Closure and an Abnormal Inflammatory Response

Authors:
Sajina Shakya (https://orcid.org/0000-0002-9400-4250) [1, 2]; shakyas2@ccf.org
Judith A. Mack (https://orcid.org/0000-0001-8935-1963) [2, 3]; mackj@ccf.org
Edward V. Maytin (https://orcid.org/0000-0002-3690-8382) [2, 3]; maytine@ccf.org

Affiliations:
[1]Department of Chemical and Biomedical Engineering, Cleveland State University, Cleveland, Ohio
[2]Department of Biomedical Engineering, Lerner Research Institute, Cleveland Clinic, Cleveland, Ohio
[3]Department of Dermatology, Dermatology & Plastic Surgery Institute, Cleveland Clinic, Cleveland, Ohio, U.S.A

Corresponding author:
Edward V. Maytin, MD, PhD
Department of Biomedical Engineering, Cleveland Clinic
Mailstop ND-20
9500 Euclid Avenue
Cleveland, OH 44195, USA
Office: 216.445.6676
Fax: 216.444.9198
E-mail: maytine@ccf.org

Short Title:
Inflammation and Wound Healing in TSG-6 null Mice

Abbreviation[i]

[i]

TSG-6	Tumor necrosis factor-stimulated gene-6
HA	Hyaluronan
HC	Heavy chain
HC-HA	HC-HA complexes
WT	Wildtype

ABSTRACT

Regulated inflammation is critical for proper wound healing. In this study, we investigated how the loss of tumor necrosis factor-stimulated gene-6 (TSG-6) affects wound closure rates and inflammatory responses in cutaneous wounds. TSG-6, by its enzymatic action, modifies hyaluronan (HA) through the transfer of heavy chain (HC) proteins from inter-α-trypsin inhibitor to HA, thereby forming HC-HA complexes. Both TSG-6 and HC-HA have been implicated as regulators of inflammation. Here we found that TSG-6 and HC-HA are constitutively expressed in normal skin, and are increased post-wounding. To understand how loss of these molecules may affect wound repair, full-thickness excisional wounds on wildtype and TSG-6 null mice were analyzed. Wound closure in TSG-6 null mice was significantly delayed relative to wildtype. In early wounds (12 h and Day 1), neutrophil recruitment was significantly delayed, whereas late wounds (Day 7) showed elevated neutrophil accumulation. Further, the pro-inflammatory cytokine TNFα and the presence of M1 proinflammatory macrophages were increased in TSG-6 null wounds compared to wildtype. Finally, reintroduction of TSG-6 into the TSG-6 null wounds rescued the delayed wound closure and the aberrant neutrophil phenotype. In summary, our study indicates that TSG-6 plays an important role in regulating inflammation during cutaneous wound repair.

INTRODUCTION

Cutaneous wound healing is a complex process that involves inflammation, keratinocyte/fibroblast proliferation, migration, angiogenesis, extracellular matrix (ECM) deposition and remodeling, all orchestrated by the specific actions of cytokines, chemokines, growth factors, and enzymes (Barrientos et al. 2008; Clark 2001; Martin 1997; Singer and Clark 1999). One of these enzymes is Tumor necrosis factor (TNF)-stimulated gene-6 (TSG-6) protein, also known as TNF–induced protein 6 (Tnfip6 or Tnfaip6). *TSG-6,* first identified by Lee et al. (Lee et al. 1990) in human foreskin fibroblasts stimulated with the pro-inflammatory cytokine TNFα, encodes a secretory glycoprotein with a molecular weight of ~30-35 kDa (Milner and Day 2003; Mittal et al. 2016; Wisniewski et al. 1993).

Functionally, TSG-6 appears to play important roles in ECM modification and in tissue inflammation. One of its important enzymatic activities is to catalyze the covalent transfer of heavy-chain (HC) protein from inter-alpha-trypsin inhibitor (IαI) and pre-α-inhibitor (PαI) to hyaluronan (HA) forming HC-HA complexes (Colon et al. 2009; Jessen and Ødum 2003; Mukhopadhyay et al. 2004). Due to this activity, TSG-6 has an important role in the stabilization and expansion of cumulus cell-oocyte complexes (COCs), a phenomenon vital for egg cell maturation, and thus accounting for female sterility in the TSG-6 null mouse (Fulop 2003; Fulop et al. 1997; Salustri et al. 1999; Salustri and Fülöp 1998). Additionally, TSG-6 protein is able to inhibit neutrophil migration via the TSG-6 Link domain (Cao et al. 2004; Getting et al. 2002) which interacts with neutrophil chemokines such as human CXCL8, and with glycosaminoglycans (GAGs) on endothelial cell surfaces (Dyer et al. 2016; Dyer et al. 2014). Furthermore, TSG-6, as well as HC-HA complexes, have been shown to promote the polarization of macrophages to an alternatively activated/ anti-inflammatory M2 phenotype instead of the classically activated/ proinflammatory

M1 phenotype (Ferrer et al. 2017; He et al. 2013; Mittal et al. 2016). Given the ability of TSG-6 to regulate the behavior of neutrophils and macrophages, we postulated that TSG-6 may be important in cutaneous wound healing. However, evidence for this prior to our study was largely indirect. Multiple investigations in other inflammatory disease models, such as rheumatoid arthritis and inflammatory colitis, suggested that TSG-6 expression is induced by inflammation and that its activity exerts anti-inflammatory effects (described more fully in the Discussion). In the skin, few previous studies on TSG-6 exist. Of those, one demonstrated the presence of TSG-6 and heavy chains HC1 and HC2 in human scars and keloids (Tan et al. 2011). Another showed that intradermal implantation of mesenchymal stem cells (MSCs) in murine skin led to TSG-6 release, faster wound healing, less fibrosis, less macrophage activation, lower TNFα levels, and reduced granulation tissue formation relative to wildtype control wounds (Qi et al. 2014). A third study investigated the effect of recombinant TSG-6 (rTSG-6) on rabbit ear wounds and showed that wounds injected with rTSG-6 healed with less hypertrophic scar than wounds receiving sham injections (Wang et al. 2015). Thus, available studies suggested that TSG-6 may play an anti-inflammatory role in cutaneous wound healing. The aim of the current study was to test this hypothesis by examining how the loss of endogenous TSG-6 affects the normal course of wound repair in a knockout mouse model (TSG-6 null). Results of such experiments, we reasoned, could provide more insight into the potential for TSG-6 as a future therapy to enhance wound healing.

RESULTS

TSG-6 protein is present in unwounded murine skin, and its expression increases post wounding

To determine the endogenous expression of TSG-6 in normal and injured skin, Western analysis was performed on proteins from intact skin and full-thickness excisional wounds of wildtype (WT) mice (Figure 1a and b). TSG-6 is constitutively expressed at low levels in unwounded skin and increases by more than 4-fold as early as 12 h post-wounding. Expression peaks by 3 days, after which it drops but remains above baseline until at least day 10 (Figure 1b). This shows that TSG-6 is upregulated after wounding, and suggests a possible functional role in wound repair.

As mentioned above, TSG-6 catalyzes the covalent transfer of HCs from IαI and pre-αI to HA, forming HC-HA complexes. HC-HA is thought to stabilize HA rich extracellular matrices, making it more adhesive to inflammatory cells (Lauer et al. 2014; Rugg et al. 2005; Zhuo et al. 2006; Zhuo et al. 2001). To quantify the levels of HC-HA in unwounded and wounded WT skin, the assay shown in Figure 1c was performed. In the absence of hyaluronidase, HC-HA complexes in the samples cannot enter the SDS-PAGE gel, and remain trapped in the well due to their large size (Figure 1c, lane 3, dashed box). However, after hyaluronidase treatment, HC-HA complexes are degraded and HC is released, appearing as a band at ~85 kDa. The presence of a HC band in the hyaluronidase-digested sample in lane 2 of Figure 1c shows that HC-HA is constitutively present in normal unwounded skin. At 3 days post-wounding, the HC band intensity increases by ~3 fold (Figure 1c, lane 4; Figure 1d). These changes mirror changes in expression of TSG-6 protein before and after wounding (Figure 1a and b).

There are no redundant enzymes that transfer HC to HA in the skin

To determine whether TSG-6 protein is the sole molecule responsible for HC-HA complex formation in skin, we assayed HC-HA in extracts from the skin of TSG-6 null mice biopsied pre- and post-wounding. The HC band normally seen in unwounded WT samples (Figure 1e, lane 2) was absent in samples from unwounded TSG-6 null skin (Figure 1e, lane 4). At Day 1 post-wounding, a time when HC-HA complexes are strongly induced in WT wounds (Figure 1e, lane 6), no HC band was detectable in TSG-6 null wounds (Figure 1e, lane 6). These data verify that the loss of TSG-6 is responsible for the inability to form HC-HA complexes, and no other molecule is induced that can compensate and transfer HC from IαI to HA. Thus, this model was appropriate for our study to understand the effect of loss of TSG-6 and HC-HA complexes on cutaneous wound healing.

The absence of TSG-6 exerts major effects upon wound closure and neutrophil infiltration

Wound closure rate is an important indicator of proper wound healing. To observe the effects of loss of TSG-6 upon cutaneous wound closure, excisional wound areas were monitored over time in WT and TSG-6 null mice (Figure 2a and b). At all the time points post-wounding, the relative wound area was larger for TSG-6 null wounds compared to WT wounds, demonstrating that loss of TSG-6 delays wound closure. Differences were statistically significant at Days 5, 7 and 10 post-wounding.

Another critical measure of proper wound healing is the orchestrated recruitment and clearance of inflammatory cells. Neutrophils are among the first to arrive at the site of injury. Interestingly, sections from early wounds (12 h and 24 h) immunostained with the neutrophilic granule marker Ly6G showed significantly fewer neutrophils in the TSG-6 null mice compared to WT mice (Figure 2c and d). However, at later time points there were more neutrophils in TSG-6

null wounds, particularly at Day 7 where the difference was highly significant (Figure 2c and d). Thus, a differential pattern of neutrophil recruitment and/or clearance was observed in the presence *versus* absence of TSG-6 (and HC-HA) in cutaneous wounds.

To evaluate macrophages, we stained wound sections using the pan macrophage marker F4/80. No significant differences in the relative number of macrophages were observed between WT and TSG-6 null wounds, suggesting that the absence of TSG-6 and HC-HA had no significant effect upon total macrophage recruitment (Figure 2e and f).

TSG-6 null mice develop an abnormally pro-inflammatory wound milieu

TSG-6 is known to have anti-inflammatory effects in other systems (Day and Milner 2018). To assess the overall inflammatory status of wounds in TSG-6 null *versus* WT mice, we evaluated levels of TNFα protein in whole wound tissue at different time points after injury, using Western analysis (Figure 3a). Consistently higher levels of TNFα expression were found in TSG-6 null wounds than in WT wounds at all time points including unwounded skin at baseline (Figure 3b). Thus, TSG-6 null wounds constitute a more pro-inflammatory environment than WT wounds. Additionally, TSG-6 has been shown to play an important role in polarization of macrophages from a pro-inflammatory M1 to anti-inflammatory M2 phenotype. To determine whether macrophages in TSG-6 null wounds might be relatively more polarized toward an M1 phenotype compared to WT macrophages, we stained Day 7 wound sections for CD38 (an M1 marker), along with F4/80, in adjacent serial sections. Evaluation of these immunostains revealed that TSG-6 null wounds contain significantly more CD38-expressing macrophages than in WT wounds (Figure 4a). Next, we assessed the level of Arginase-1 (Arg1, an M2 marker) in whole wounds (Figure 4c), both by immunostaining (Fig. 4b) and by western analysis (Figure 4e). We found that Arg1 is consistently

lower in TSG-6 null wounds at all time points evaluated, again suggesting a more pro-inflammatory environment in TSG-6 null wounds. To focus more closely upon the expression of M1/M2 phenotypic markers in the macrophages themselves, single cells were isolated from Day 5 wounds by dispase/collagenase digestion, followed by flow cytometric analysis of macrophages. We found that in TSG-6 null mice, a higher proportion of F4/80 positive macrophages expressed TNFα (a well-established M1 marker), while the proportion of macrophages expressing Arg1 was lower, relative to WT wounds (Figure 4d and e). Thus, the absence of TSG-6 in null wounds results in polarization of the overall macrophage population to a more proinflammatory phenotype.

Reintroduction of recombinant TSG-6 into TSG-6 knockout wounds restores normal healing

To confirm that the difference in wound closure observed in WT versus TSG-6 null wounds was due to the loss of TSG-6, a protein rescue experiment was performed. Recombinant TSG-6 protein (rTSG-6) was reintroduced at two time points, i.e., immediately after wounding (Day 0) and at 4 days post-wounding (Figure 5a). In TSG-6 null mice, wound sizes trended slightly lower at Days 1-5 in wounds receiving the rTSG-6 injections, and became significantly smaller (and equal to control WT wounds) at Day 7 (Figure 5b and c). Interestingly, injection of rTSG-6 into WT wounds worsened wound closure compared to the WT vehicle control. These findings suggested that the delay in wound closure in TSG-6 null wounds is attributable to loss of TSG-6.

To confirm that differences in neutrophil recruitment between WT and TSG-6 null wounds were also due to loss of TSG-6, a similar TSG-6 reintroduction experiment was performed. The experimental scheme was essentially the same as Figure 5a, but now wounds were harvested (either at 12 h or Day 7). Sections were immunostained for Ly6G. The number of neutrophils at the wound site at 12 h post wounding, which was reduced in TSG-6 null mice relative to WT, was significantly

increased after one injection of rTSG-6 becoming similar to WT (however, WT wounds receiving rTSG-6 showed some delay in neutrophil recruitment) (Figure 5d). Likewise, the number of neutrophils observed in Day 7 wounds, ordinarily much higher in TSG-6 null wounds, was completely normalized to WT levels in mice receiving two rTSG-6 injections (Figure 5e). Thus, the differential neutrophil recruitment observed in TSG-6 null wounds is reversible when TSG-6 is restored in the skin.

DISCUSSION

This study describes abnormal wound healing responses in mice lacking TSG-6, the enzyme that catalyzes cross-linking of heavy chain proteins to hyaluronan. Our overall findings show that relative to WT controls, TSG-6 null wounds display (i) delayed wound closure, (ii) delayed neutrophil recruitment in early wounds, (iii) exacerbated neutrophil recruitment in late wounds, and (iv) polarization of wound macrophages toward a pro-inflammatory ("M1") phenotype. Reintroduction of recombinant TSG-6 can reverse both the delayed wound closure and the abnormal neutrophil recruitment.

Our study was motivated by previous literature suggesting an important role for TSG-6 in regulation of inflammation. In many cell and tissue types, TSG-6 expression is low or absent under normal condtions, but stimulated by pro-inflammatory factors such as TNFα, interleukin-1 (IL-1), and lipopolysaccharide (LPS) (Milner and Day 2003). Here we show that TSG-6 is constitutively expressed at low levels in unwounded mouse skin, in agreement with earlier findings in human skin (Tan et al. 2011). However, TSG-6 expression is greatly increased after wounding. Similarly, HC-HA complexes are detectable in low amounts in normal skin and become significantly elevated after wounding. HC-HA is completely absent in the skin of TSG-6 null mice. Therefore, levels of TSG-6 appear to correlate with levels of its enzymatic product, HC-HA. Regarding wound inflammation, results reported after injection of rTSG-6 or MSCs (which produce TSG-6 along with many other factors) in other inflammatory models such as murine experimental arthritis (Bardos et al. 2001), myocardial infarction (Lee et al. 2009), DSS-induced colitis (Sala et al. 2015), and rabbit ear wounds (Wang et al. 2015), indicated that TSG-6 might have an anti-inflammatory role, resulting in decreased disease activity and/or improved recovery. In accordance with these studies, we found that absence of endogenous TSG-6 is deleterious to wound healing whereas restoration of the

protein through direct dermal injection of rTSG-6 into TSG-6 null mouse wounds restored normal wound healing, at least in terms of the parameters evaluated here.

Beyond identifying a new wound-delay phenotype, our study provides several insights about inflammation and TSG-6 in wounds. Total loss of TSG-6 results in exacerbated pro-inflammatory effects in healing wounds. As a brief review, wounding initiates the release of multiple proinflammatory factors that stimulate local recruitment of neutrophils and monocytes into the wound bed (Martin and Leibovich 2005; Singer and Clark 1999; Wang 2018). Neutrophil recruitment starts as early as 4 h post-wounding and plateaus around 3 days (Kim et al. 2008). Studies in other models in which rTSG-6 protein was injected into inflamed tissue revealed a decreased inflammatory response, including reductions in pro-inflammatory cytokines and neutrophil infiltration (Beltran et al. 2015; Kim et al. 2014; Oh et al. 2010); absence of TSG-6 on the other hand led to increased neutrophil infiltration (Szanto et al. 2004).

Interestingly, in our TSG-6 null wound model the neutrophil recruitment response appears to be biphasic. At early timepoints (12 and 24 h post-wounding), neutrophils are significantly lower in TSG-6 null wounds than in WT wounds. To explain this, we postulate an interaction between neutrophils and HC-HA on the endothelial glycocalyx. It is known that the luminal side (endothelium) of blood vessels is lined with an HA rich glycocalyx (Reitsma et al. 2007; Shakya et al. 2015), which we hypothesize under wound conditions becomes decorated with HC, forming HC-HA complexes. Because leukocytes bind more avidly to HC-HA complexes than to non-complexed HA (Lauer et al. 2014; Zhuo et al. 2006), HC-HA should facilitate neutrophil attachment within small vessels in the wound bed in WT wounds. Thus, the absence of HC-HA in TSG-6 null wounds should delay neutrophil recruitment in early wounds. However, in later wounds, mechanisms of neutrophil recruitment appear to be different since there is a relatively higher number of neutrophils

in TSG-6 null wounds as compared to WT. The excessive levels of pro-inflammatory TNFα in TSG-6 null wounds may be one contributor to neutrophil overabundance especially at Day 7 where levels of TNFα and neutrophils are significantly higher in TSG-6 null wounds. TNFα elevation in TSG-6 deficient mice might occur via several mechanisms, e.g. through feedback inhibition pathways that become de-repressed upon loss of TSG-6, or via the action of cytokines released by incoming macrophages that stimulate cells in the wound bed to synthesize TNFα. Regardless of the recruitment mechanism, excessive neutrophil activity has been tied to delayed wound healing (Kim et al. 2008; Wilgus et al. 2013), and is therefore a likely contributor to the aberrant wound healing observed in TSG-6 null mice.

Macrophages, the other major inflammatory cell type in wounds, remove apoptotic neutrophil debris and also secrete pro-inflammatory and anti-inflammatory cytokines, depending upon the particular macrophage phenotype (Koh and DiPietro 2011; Larouche et al. 2018; Wilgus et al. 2013). Although we found no significant difference in the absolute number of macrophages in TSG-6 null *versus* WT wounds, we did determine that macrophages in TSG-6 null wounds were skewed towards an M1 phenotype. This is in agreement with previous studies showing that TSG-6 and immobilized HC-HA complexes can drive macrophages to a more anti-inflammatory phenotype (Ferrer et al. 2017; He et al. 2013; Mittal et al. 2016), and that TSG-6-producing MSCs can lower proinflammatory marker expression and increase anti-inflammatory M2 macrophages in a colitis model (Song et al. 2017). From several lines of evidence, including the fact that M2 macrophages are known to promote tissue repair, and that M1 macrophages are greatly increased in chronic wounds such as diabetic ulcers, it is becoming clear that controlled regulation of macrophage phenotype is critical for proper wound healing (Hesketh et al. 2017; Khanna et al. 2010; Krzyszczyk et al. 2018). Thus, we conclude that TSG-6 plays a crucial role in regulating macrophage

phenotypes during cutaneous wound healing and this dysregulation in M1/M2 ratio in null wounds could be contributing to aberrant healing.

An additional factor to mention, because it could potentially contribute to the observed phenotypes, is an ability of TSG-6 to regulate chemokine function. As shown by Dyer et al., TSG-6 can regulate chemokine availability by competitive binding to various chemokines and/or sulfated GAGs in the ECM (Dyer et al. 2016; Dyer et al. 2014). Absence of TSG-6 might interrupt some of these interactions and depending upon which cytokines are affected, could influence neutrophil migration. This possible mechanism would make an interesting subject for future investigation.

A strength of the current study is that TSG-6 restoration (rTSG-6 injection into TSG-6 deficient wounds) was shown to normalize wound closure and neutrophil recruitment. These results unambiguously establish that the defects observed in TSG-6 null mice result from loss of TSG-6 protein. Interestingly, while reintroduction of rTSG-6 into TSG-6 null wounds reversed the wound delay and neutrophil recruitment defects, addition of rTSG-6 into normal WT wounds worsened both of these phenomena. Apparently, tight regulation of TSG-6 is critical for proper wound healing, and either excessive or insufficient amounts are deleterious.

In summary, loss of TSG-6 leads to abnormal pro-inflammatory changes and is detrimental to wound healing, whereas a regulated amount of TSG-6 is crucial for a normal inflammatory response and proper wound closure. While more studies are needed to fully elucidate the mechanisms behind the phenotypes observed, our study provides important groundwork for understanding the role of endogenous TSG-6 in cutaneous wound healing.

MATERIALS AND METHODS

Animals

C57BL/6J mice were obtained from JAX Laboratories (Bar Harbor, ME). TSG-6 null mice, whose generation was described by Fülöp et al. (Fulop 2003), was generously provided by Dr. Mark Aronica in our institute. Mice were maintained per guidelines of the American Association for the Accreditation of Laboratory Animal Care. All procedures were approved by the Cleveland Clinic Institutional Animal Care and Use Committee (IACUC).

Wounding experiments

Mice (8–10 weeks old) were anesthetized via intraperitoneal Ketamine-Xylazine injection, and the upper back shaved with an electric razor. The next day, two full-thickness excisional wounds were made using 5 mm punch biopsies (Acuderm, Fort Lauderdale, FL) under anesthesia. To follow wound closure, mice were anesthetized with isofluorane and photographed from a fixed distance using a digital camera. Wound area was determined from the photos using standard imaging software. For histological examination, wound tissues were harvested at defined time points, fixed in Histochoice (Amresco, Solon, OH), and paraffin embedded. Other wound tissues were flash frozen in liquid nitrogen and stored at -80 °C for subsequent protein and RNA isolation.

Western Blotting

Protein lysates were prepared from wound samples as described previously (Mack and Maytin 2010). Lysates were electrophoresed in NuPage 4-12 % Bis-Tris gels (Invitrogen, Carlsbad, CA), blotted onto PVDF membranes (Millipore, Burlington, MA), and probed overnight (4 °C) with one of the following primary antibodies: Anti-TSG-6 mouse monoclonal (1 μg/ml;

Millipore); rat monoclonal TNFα (1 μg/ml; BioXCell, West Lebanon, NH); rabbit monoclonal Arg1 (1:1000, Cell Signaling Technology, Danvers, MA); rabbit anti-mouse Actin (1:1000; Santa Cruz Biotechnology, Dallas, TX). This was followed by 1.5 hour incubation with appropriate horseradish peroxidase (HRP)-conjugated secondary antibodies (1:10,000; Jackson ImmunoResearch, West Grove, PA). Chemiluminescent detection was performed using Amersham™ ECL™, or ECL™ Prime reagent kits (GE Healthcare, Chicago, IL). Protein bands were quantified using IPLab Spectrum imaging software (Scanalytics, Rockville, MD).

Evaluation of HC modification of hyaluronan (HC-HA analysis)

HC-HA analyses were performed as described (Lauer et al. 2015). Briefly, skin tissues were collected, weighed and minced in PBS at 1 μl volume per 0.33 mg of tissue. *Streptomyces* hyaluronidase (Millipore) was added (20 TRU/ml for extraction of HCs, or equal volumes of PBS for No-hyaluronidase controls), incubated for 30 min on wet ice followed by 30 min at 37 °C. After centrifugation (13,000 rpm), supernatants were collected, electrophoresed, and blotted. Blots were incubated with anti-IαI rabbit polyclonal Dako antibody (1:8000; Agilent Technologies, Santa Clara, CA), followed by IRDye® 800CW donkey anti-rabbit secondary (1:15,000; LI-COR Biosciences, Licoln, NE). Blots were imaged on an Odyssey infrared imaging system (LI-COR Biosciences).

Immunostaining for neutrophils and macrophages

Paraffin embedded tissues were cut (5-micron sections), rehydrated, blocked with 3% normal goat serum for 30 min. Sections were incubated overnight (4 °C) with the respective primary antibodies: Anti-Ly6G rat monoclonal (1:100; Affymetrix, Santa Clara, CA) for neutrophils; Anti F4/80 rat monoclonal (1:100; Bio-Rad, Hercules, CA) for macrophages. A biotinylated

goat anti-rat biotin secondary (1:300) was followed by Vectastain ABC reagent (Vector Laboratories, Burlingame, CA) for 30 minutes each. After detection using a DAB peroxidase substrate kit, mounted slides were scanned using an Aperio AT2 slide-scanner (Leica Biosystems, Buffalo Grove, IL). Areas positively stained for neutrophils or macrophages were evaluated using IPLab software (Scanalytics).

Immunostaining for macrophages phenotypes

Serial wound sections were incubated overnight (4 °C) with the respective primary antibodies: rabbit anti-mouse CD38 (1:100; Bioss, Woburn, MA) for M1 macrophages; rat monoclonal F4/80 (1:100; Bio-Rad) for all macrophages; rabbit monoclonal Arg1 (1:100; Cell Signaling Technology) for M2 macrophages. Sections were then incubated with goat anti-rat or goat anti-rabbit biotinylated secondary antibody (1:300; 30 min; Vector Laboratories) followed by incubation with Alexa Fluor 488 Streptavidin (1:500; 1.5 hour, Invitrogen), and mounted in VECTASHEILD mounting medium (Vector).

Flow cytometry for M1 and M2 macrophages

Single cell suspensions from Day 5 wounds were prepared as described (Bannon et al. 2013) with modifications. Briefly, wounds were isolated from WT and TSG-6 null animals and weighed. Tissues were rinsed once each in 70 % ethanol and PBS, cut into 2 mm^2 pieces and incubated overnight (4 ºC) in 20 µl HBSS per mg of wound tissue with 1 mg/mL Dispase II (Sigma-Aldrich, St. Louis, MO), 3% FBS and 10 mg/mL G418 (Sigma-Aldrich). Tissues were transferred to 80 µl HBSS per mg wound tissue with 1 mg/mL Collagenase I (Worthington, Lakewood, NJ), 75 U/mL DNaseI (Worthington) and 5 mg/mL G418, and incubated for 2 hours (37 ºC) with shaking. Cell suspensions were filtered through a 40 µm cell strainer (Corning

Technology, Corning, NY) and washed twice with PBS buffer (PBS, 3% FBS, 0.1 mM EDTA), and centrifuged at 400 rpm. Cells were counted, resuspended at 1 million cells/ml in PBS buffer, and labeled with fluorescently tagged antibodies: Rat anti-mouse CD45 (1:200); rat anti-mouse F4/80 (1:80); rat anti-mouse TNFα (1:40; BioLegend, San Diego, CA); sheep anti-mouse Arg1 (1:10; Novus Biologicals, Centennial, CO) for 25 minutes (4 ºC). Samples were analyzed on a BD LSRFortessa flow analyzer (BD Biosciences, Mississauga, ON, Canada).

Recombinant TSG-6 injection

Mice were shaved, anesthetized, and two full thickness excisional wounds made using 5 mm punch biopsies. The edges and center of each wound was injected using an insulin syringe, with 2 µg of recombinant human TSG-6 (rTSG-6, R&D Systems, Minneapolis, MN) in 100 µl PBS (or with PBS alone) immediately after wounding and at Day 4 post wounding. Wounds were photographed to evaluate closure. Some wounds were collected at 12 h or Day 7 post wounding to evaluate neutrophil and macrophage infiltration.

Statistical analysis

All statistical analyses were performed using a two-tailed Student's t-test. A p-value < 0.05 was considered statistically significant.

DATA AVAILABILITY STATEMENT

No datasets were generated or analyzed during the current study.

CONFLICT OF INTEREST

The authors state no conflict of interest.

ACKNOWLEDGEMENTS

We thank Dr. Mark Aronica for sharing the C57BL/6 TSG-6 null mice. We acknowledge Kewal Asosingh, PhD, and the Flow Cytometry Core of the Lerner Research Institute, Cleveland Clinic, for their help in Flow Cytometry data analysis. We acknowledge the teaching and contributions of the late Mark Lauer, Ph.D.

This work was supported by grant P01 HL107147 from NIH/NHLBI.

REFERENCES

Bannon P, Wood S, Restivo T, Campbell L, Hardman MJ, Mace KA. Diabetes induces stable intrinsic changes to myeloid cells that contribute to chronic inflammation during wound healing in mice. Dis. Model. Mech. 2013;6(6):1434–47

Bardos T, Kamath RV, Mikecz K, Glant TT. Anti-inflammatory and chondroprotective effect of TSG-6 (tumor necrosis factor-alpha-stimulated gene-6) in murine models of experimental arthritis. Am. J. Pathol. 2001;159(5):1711–21

Barrientos S, Stojadinovic O, Golinko MS, Brem H, Tomic-Canic M. PERSPECTIVE ARTICLE: Growth factors and cytokines in wound healing: Growth factors and cytokines in wound healing. Wound Repair Regen. 2008;16(5):585–601

Beltran SR, Svoboda KK, Kerns DG, Sheth A, Prockop DJ. Anti-inflammatory protein tumor necrosis factor-alpha-stimulated protein 6 (TSG-6) promotes early gingival wound healing: an in vivo study. J. Periodontol. 2015;86(1):62–71

Cao TV, La* M, Getting* SJ, Day AJ, Perretti* M. Inhibitory Effects of TSG-6 Link Module on Leukocyte–Endothelial Cell Interactions *In Vitro* and *In Vivo*. Microcirculation. 2004;11(7):615–24

Clark RA. Fibrin and wound healing. Ann. N. Y. Acad. Sci. 2001;936(Journal Article):355–67

Colon E, Shytuhina A, Cowman MK, Band PA, Sanggaard KW, Enghild JJ, et al. Transfer of inter-alpha-inhibitor heavy chains to hyaluronan by surface-linked hyaluronan-TSG-6 complexes. J. Biol. Chem. 2009;284(4):2320–31

Day AJ, Milner CM. TSG-6: A multifunctional protein with anti-inflammatory and tissue-protective properties. Matrix Biol. 2018; Available from: https://linkinghub.elsevier.com/retrieve/pii/S0945053X17304730

Dyer DP, Salanga CL, Johns SC, Valdambrini E, Fuster MM, Milner CM, et al. The Anti-inflammatory Protein TSG-6 Regulates Chemokine Function by Inhibiting Chemokine/Glycosaminoglycan Interactions. J. Biol. Chem. 2016;291(24):12627–40

Dyer DP, Thomson JM, Hermant A, Jowitt TA, Handel TM, Proudfoot AE, et al. TSG-6 inhibits neutrophil migration via direct interaction with the chemokine CXCL8. J. Immunol. Baltim. Md 1950. 2014;192(5):2177–85

Ferrer RA, Saalbach A, Grünwedel M, Lohmann N, Forstreuter I, Saupe S, et al. Dermal Fibroblasts Promote Alternative Macrophage Activation Improving Impaired Wound Healing. J. Invest. Dermatol. 2017;137(4):941–50

Fulop C. Impaired cumulus mucification and female sterility in tumor necrosis factor-induced protein-6 deficient mice. Development. 2003;130(10):2253–61

Fulop C, Kamath RV, Li Y, Otto JM, Salustri A, Olsen BR, et al. Coding sequence, exon-intron structure and chromosomal localization of murine TNF-stimulated gene 6 that is specifically expressed by expanding cumulus cell-oocyte complexes. Gene. 1997;202(1–2):95–102

Getting SJ, Mahoney DJ, Cao T, Rugg MS, Fries E, Milner CM, et al. The Link Module from Human TSG-6 Inhibits Neutrophil Migration in a Hyaluronan- and Inter-α-inhibitor-independent Manner. J. Biol. Chem. 2002;277(52):51068–76

He H, Zhang S, Tighe S, Son J, Tseng SCG. Immobilized Heavy Chain-Hyaluronic Acid Polarizes Lipopolysaccharide-activated Macrophages toward M2 Phenotype. J. Biol. Chem. 2013;288(36):25792–803

Hesketh M, Sahin KB, West ZE, Murray RZ. Macrophage Phenotypes Regulate Scar Formation and Chronic Wound Healing. Int. J. Mol. Sci. 2017;18(7):1545

Jessen TE, Ødum L. Role of tumour necrosis factor stimulated gene 6 (TSG-6) in the coupling of inter-alpha-trypsin inhibitor to hyaluronan in human follicular fluid. Reprod. Camb. Engl. 2003;125(1):27–31

Khanna S, Biswas S, Shang Y, Collard E, Azad A, Kauh C, et al. Macrophage Dysfunction Impairs Resolution of Inflammation in the Wounds of Diabetic Mice. Vij N, editor. PLoS ONE. 2010;5(3):e9539

Kim J-A, Ko JH, Ko AY, Lee HJ, Kim MK, Wee WR, et al. TSG-6 Protects Corneal Endothelium From Transcorneal Cryoinjury in Rabbits. Investig. Opthalmology Vis. Sci. 2014;55(8):4905

Kim M-H, Liu W, Borjesson DL, Curry F-RE, Miller LS, Cheung AL, et al. Dynamics of Neutrophil Infiltration during Cutaneous Wound Healing and Infection Using Fluorescence Imaging. J. Invest. Dermatol. 2008;128(7):1812–20

Koh TJ, DiPietro LA. Inflammation and wound healing: the role of the macrophage. Expert Rev. Mol. Med. 2011;13 Available from: http://www.journals.cambridge.org/abstract_S1462399411001943

Krzyszczyk P, Schloss R, Palmer A, Berthiaume F. The Role of Macrophages in Acute and Chronic Wound Healing and Interventions to Promote Pro-wound Healing Phenotypes. Front. Physiol. 2018;9 Available from: http://journal.frontiersin.org/article/10.3389/fphys.2018.00419/full

Larouche J, Sheoran S, Maruyama K, Martino MM. Immune Regulation of Skin Wound Healing: Mechanisms and Novel Therapeutic Targets. Adv. Wound Care. 2018;7(7):209–31

Lauer ME, Aytekin M, Comhair SA, Loftis J, Tian L, Farver CF, et al. Modification of Hyaluronan by Heavy Chains of Inter-α-Inhibitor in Idiopathic Pulmonary Arterial Hypertension. J. Biol. Chem. 2014;289(10):6791–8

Lauer ME, Loftis J, de la Motte C, Hascall VC. Analysis of the heavy-chain modification and TSG-6 activity in pathological hyaluronan matrices. Methods Mol. Biol. Clifton NJ. 2015;1229(Journal Article):543–8

Lee TH, Lee GW, Ziff EB, Vilcek J. Isolation and characterization of eight tumor necrosis factor-induced gene sequences from human fibroblasts. Mol. Cell. Biol. 1990;10(5):1982–8

Lee RH, Pulin AA, Seo MJ, Kota DJ, Ylostalo J, Larson BL, et al. Intravenous hMSCs Improve Myocardial Infarction in Mice because Cells Embolized in Lung Are Activated to Secrete the Anti-inflammatory Protein TSG-6. Cell Stem Cell. 2009;5(1):54–63

Mack JA, Maytin EV. Persistent Inflammation and Angiogenesis during Wound Healing in K14-Directed Hoxb13 Transgenic Mice. J. Invest. Dermatol. 2010;130(3):856–65

Martin P. Wound Healing--Aiming for Perfect Skin Regeneration. Science. 1997;276(5309):75–81

Martin P, Leibovich SJ. Inflammatory cells during wound repair: the good, the bad and the ugly. Trends Cell Biol. 2005;15(11):599–607

Milner CM, Day AJ. TSG-6: a multifunctional protein associated with inflammation. J. Cell Sci. 2003;116(Pt 10):1863–73

Mittal M, Tiruppathi C, Nepal S, Zhao Y-Y, Grzych D, Soni D, et al. TNFα-stimulated gene-6 (TSG6) activates macrophage phenotype transition to prevent inflammatory lung injury. Proc. Natl. Acad. Sci. 2016;113(50):E8151–8

Mukhopadhyay D, Asari A, Rugg MS, Day AJ, Fülöp C. Specificity of the tumor necrosis factor-induced protein 6-mediated heavy chain transfer from inter-alpha-trypsin inhibitor to hyaluronan: implications for the assembly of the cumulus extracellular matrix. J. Biol. Chem. 2004;279(12):11119–28

Oh JY, Roddy GW, Choi H, Lee RH, Ylostalo JH, Rosa RH, et al. Anti-inflammatory protein TSG-6 reduces inflammatory damage to the cornea following chemical and mechanical injury. Proc. Natl. Acad. Sci. 2010;107(39):16875–80

Qi Y, Jiang D, Sindrilaru A, Stegemann A, Schatz S, Treiber N, et al. TSG-6 released from intradermally injected mesenchymal stem cells accelerates wound healing and reduces tissue fibrosis in murine full-thickness skin wounds. J. Invest. Dermatol. 2014;134(2):526–37

Reitsma S, Slaaf DW, Vink H, van Zandvoort MAMJ, oude Egbrink MGA. The endothelial glycocalyx: composition, functions, and visualization. Pflüg. Arch. - Eur. J. Physiol. 2007;454(3):345–59

Rugg MS, Willis AC, Mukhopadhyay D, Hascall VC, Fries E, Fülöp C, et al. Characterization of Complexes Formed between TSG-6 and Inter-α-inhibitor That Act as Intermediates in the Covalent Transfer of Heavy Chains onto Hyaluronan. J. Biol. Chem. 2005;280(27):25674–86

Sala E, Genua M, Petti L, Anselmo A, Arena V, Cibella J, et al. Mesenchymal Stem Cells Reduce Colitis in Mice via Release of TSG6, Independently of Their Localization to the Intestine. Gastroenterology. 2015;149(1):163-176.e20

Salustri A, Camaioni A, Di Giacomo M, Fulop C, Hascall VC. Hyaluronan and proteoglycans in ovarian follicles. Hum. Reprod. Update. 1999;5(4):293–301

Salustri A, Fülöp C. Role of hyaluronan during ovulation and fertilisation. 1998; Available from: http://glycoforum.gr.jp/science/hyaluronan/HA03/HA03E.html

Shakya S, Wang Y, Mack JA, Maytin EV. Hyperglycemia-Induced Changes in Hyaluronan Contribute to Impaired Skin Wound Healing in Diabetes: Review and Perspective. Int. J. Cell Biol. 2015;2015:1–11

Singer AJ, Clark RA. Cutaneous wound healing. N. Engl. J. Med. 1999;341(10):738–46

Song W-J, Li Q, Ryu M-O, Ahn J-O, Ha Bhang D, Chan Jung Y, et al. TSG-6 Secreted by Human Adipose Tissue-derived Mesenchymal Stem Cells Ameliorates DSS-induced colitis by Inducing M2 Macrophage Polarization in Mice. Sci. Rep. 2017;7(1) Available from: http://www.nature.com/articles/s41598-017-04766-7

Szanto S, Bardos T, Gal I, Glant TT, Mikecz K. Enhanced neutrophil extravasation and rapid progression of proteoglycan-induced arthritis in TSG-6-knockout mice. Arthritis Rheum. 2004;50(9):3012–22

Tan KT, McGrouther DA, Day AJ, Milner CM, Bayat A. Characterization of hyaluronan and TSG-6 in skin scarring: differential distribution in keloid scars, normal scars and unscarred skin. J. Eur. Acad. Dermatol. Venereol. JEADV. 2011;25(3):317–27

Wang J. Neutrophils in tissue injury and repair. Cell Tissue Res. 2018;371(3):531–9

Wang H, Chen Z, Li XJ, Ma L, Tang YL. Anti-inflammatory cytokine TSG-6 inhibits hypertrophic scar formation in a rabbit ear model. Eur. J. Pharmacol. 2015;751(Journal Article):42–9

Wilgus TA, Roy S, McDaniel JC. Neutrophils and Wound Repair: Positive Actions and Negative Reactions. Adv. Wound Care. 2013;2(7):379–88

Wisniewski HG, Maier R, Lotz M, Lee S, Klampfer L, Lee TH, et al. TSG-6: a TNF-, IL-1-, and LPS-inducible secreted glycoprotein associated with arthritis. J. Immunol. Baltim. Md 1950. 1993;151(11):6593–601

Zhuo L, Kanamori A, Kannagi R, Itano N, Wu J, Hamaguchi M, et al. SHAP Potentiates the CD44-mediated Leukocyte Adhesion to the Hyaluronan Substratum. J. Biol. Chem. 2006;281(29):20303–14

Zhuo L, Yoneda M, Zhao M, Yingsung W, Yoshida N, Kitagawa Y, et al. Defect in SHAP-Hyaluronan Complex Causes Severe Female Infertility: A study by inactivation of the bikunin gene in mice. J. Biol. Chem. 2001;276(11):7693–6

FIGURE LEGENDS

Figure 1. ***TSG-6 protein and HC-HA are present in unwounded murine skin and both are significantly increased post wounding; HC-HA is absent in TSG-6 null unwounded and wounded skin.*** (a) TSG-6 western blots in unwounded and wounded skin. Actin, loading control. (b) Densitometric quantification of multiple TSG-6 western blots. *Numbers above bars*, wounds analyzed. (c) Analysis of HC-HA on acrylamide gels. HC protein present in HC-HA complexes (*boxed band*, Lane 3) are released using *Streptomyces* hyaluronidase (Hy'ase). HC-HA levels are increased in wounds (Lane 4) relative to unwounded skin (Lane 2). (d) Quantification of HC-HA complexes from 1c. (e) HC-HA assay of unwounded skin and Day 1 excisional wounds. WT skin showed the presence of a HC band in the hyaluronidase-treated sample which was greater after wounding (*blue boxes*). TSG-6 null samples lacked a HC band, either before or after wounding (*dashed red boxes*). *Error bars= Mean ± SEM.*

Figure 2. ***Loss of TSG-6 results in delayed wound closure and abnormal neutrophil recruitment.*** (a) Full-thickness excisional wounds in WT and TSG-6 null mice. (b) Quantification of wound area using IPLab imaging software. Wound sizes are represented as a percentage of their original size. *Closed circles*, TSG-6 null. *Open circles,* WT. For each timepoint N= 20, except for day 10, N= 10. (c) Neutrophil staining of WT and TSG-6 null wounds. (d) Quantification of neutrophil density using IPLab. Neutrophil recruitment was delayed in early wounds (12 h and 24 h), while recruitment was exacerbated at Day 7. (e) Macrophage-specific staining of WT and TSG-6 null wounds. (f) Quantification of macrophage density; no significant differences were observed between TSG-6 null and WT wounds at Days 5 and 7. *Scale bars= 100 µm; Error bars= Mean ± SEM.*

Figure 3. ***Absence of TSG-6 leads to a more pro-inflammatory wound milieu.*** (a) Harvested WT and TSG-6 null skin samples (unwounded and wounded) were analyzed via Western blotting. Actin, loading control. *w, WT; n, TSG-6 null.* (b) Quantification of multiple experiments; TNFα expression was relatively higher in TSG-6 null wounds at all time points, including unwounded skin. Differences were significant at 12 h and Day 7 post-wounding. *Error bars= Mean ± SEM.*

Figure 4. ***Loss of TSG-6 polarizes cutaneous macrophages toward a pro-inflammatory phenotype.*** (a) Serial sections from WT and TSG-6 null Day 7 wounds stained with an M1 macrophage (CD38) marker, or with a pan-macrophage marker (F4/80). The ratio of CD38 to F4/80 positive cells was significantly higher in TSG-6 null wounds. (b) Serial sections from WT and TSG-6 null Day 7 wounds stained for an M2 macrophage (Arg1) marker or a pan-macrophage marker (F4/80). The ratio of Arg1 to F4/80 positive cells was significantly lower in the TSG-6 null wounds. (c) Western blot and quantification of Arg1 expression in TSG-6 null *versus* WT wounds. *w,* WT; *n,* TSG-6 null. (d, e) Flow cytometric analyses of macrophages in single cell suspensions obtained from Day 5 WT (d) and TSG-6 null wounds (e). *Error bars= Mean ± SEM.*

Figure 5. ***Re-introduction of recombinant TSG-6 (rTSG-6) into TSG-6 null wounds rescues the delayed closure and abnormal neutrophil recruitment.*** (a) Schematic diagram showing the location of rTSG-6 injections (red x's). Wounds were injected with PBS (vehicle) alone, or with rTSG-6 in PBS. (b) Photos of TSG-6 null wounds +/- rTSG-6. (c) Quantification of Day 7 wound areas in WT and TSG-6 null mice +/- rTSG-6. Wound sizes are represented as percentage

of initial area. (d) Neutrophil staining of wounds at 12 h showed that the delay in neutrophil recruitment in TSG-6 null wounds was partially rescued by rTSG-6 injections. A non-significant delay in neutrophil recruitment was observed in WT + rTSG-6. (e) Neutrophil staining of Day 7 wounds showed that the exacerbated neutrophil recruitment was completely reversed by rTSG-6 treatment. *Scale bars= 100 µm; Error bars= Mean ± SEM.*

Figure 1.

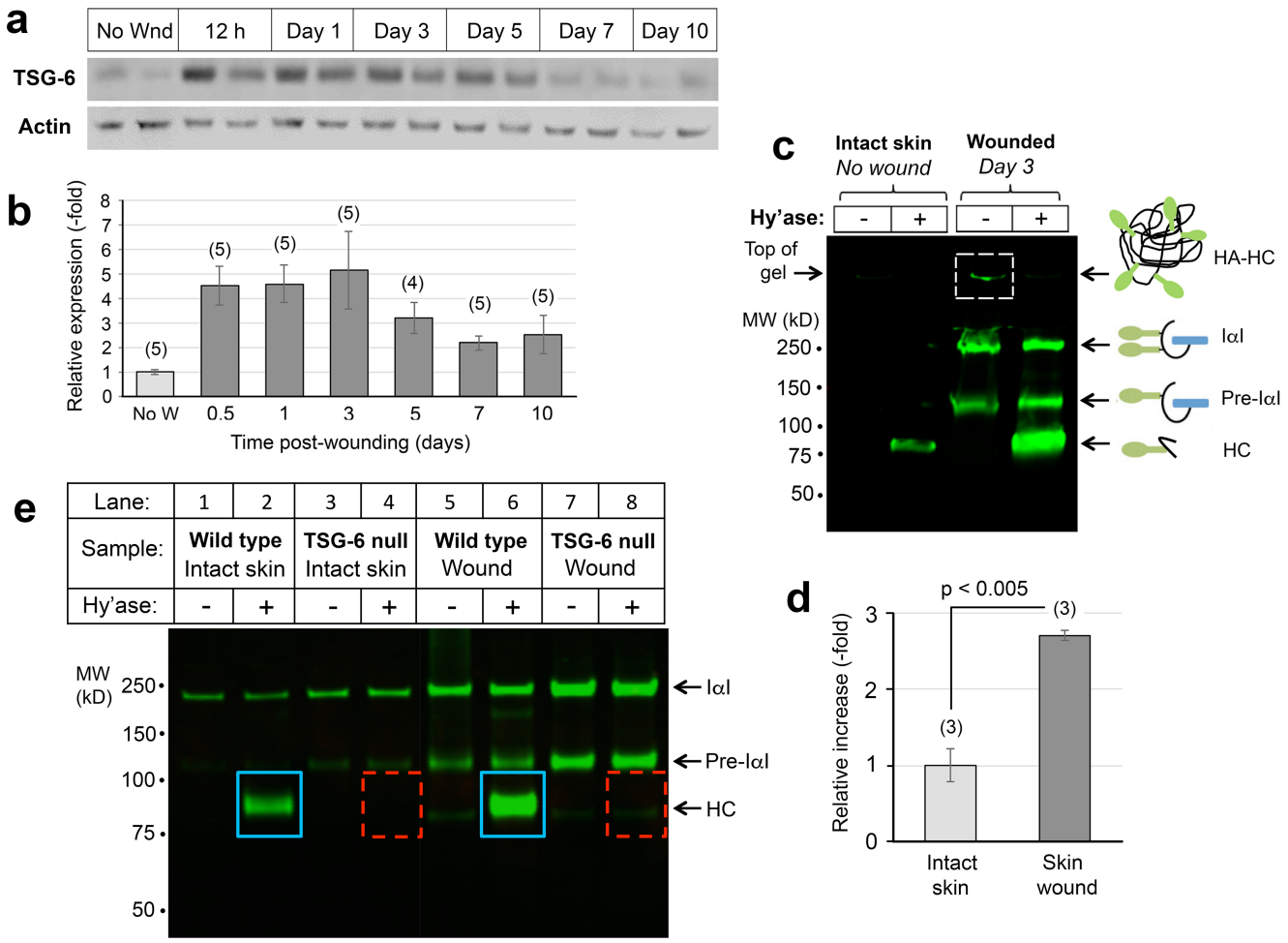
a
No Wnd
12 h
Day 1
Day 3
Day 5
Day 7
Day 10
TSG-6
Actin
b
Relative expression (-fold)
Time post-wounding (days)
No W
0.5
1
3
5
7
10
c
Intact skin
No wound
Wounded
Day 3
Hy'ase:
Top of gel
MW (kD)
250
150
100
75
50
HA-HC
IαI
Pre-IαI
HC
d
p < 0.005
Relative increase (-fold)
Intact skin
Skin wound
e
Lane:
Sample:
Wild type Intact skin
TSG-6 null Intact skin
Wild type Wound
TSG-6 null Wound
Hy'ase:
MW (kD)
IαI
Pre-IαI
HC

Figure 2.

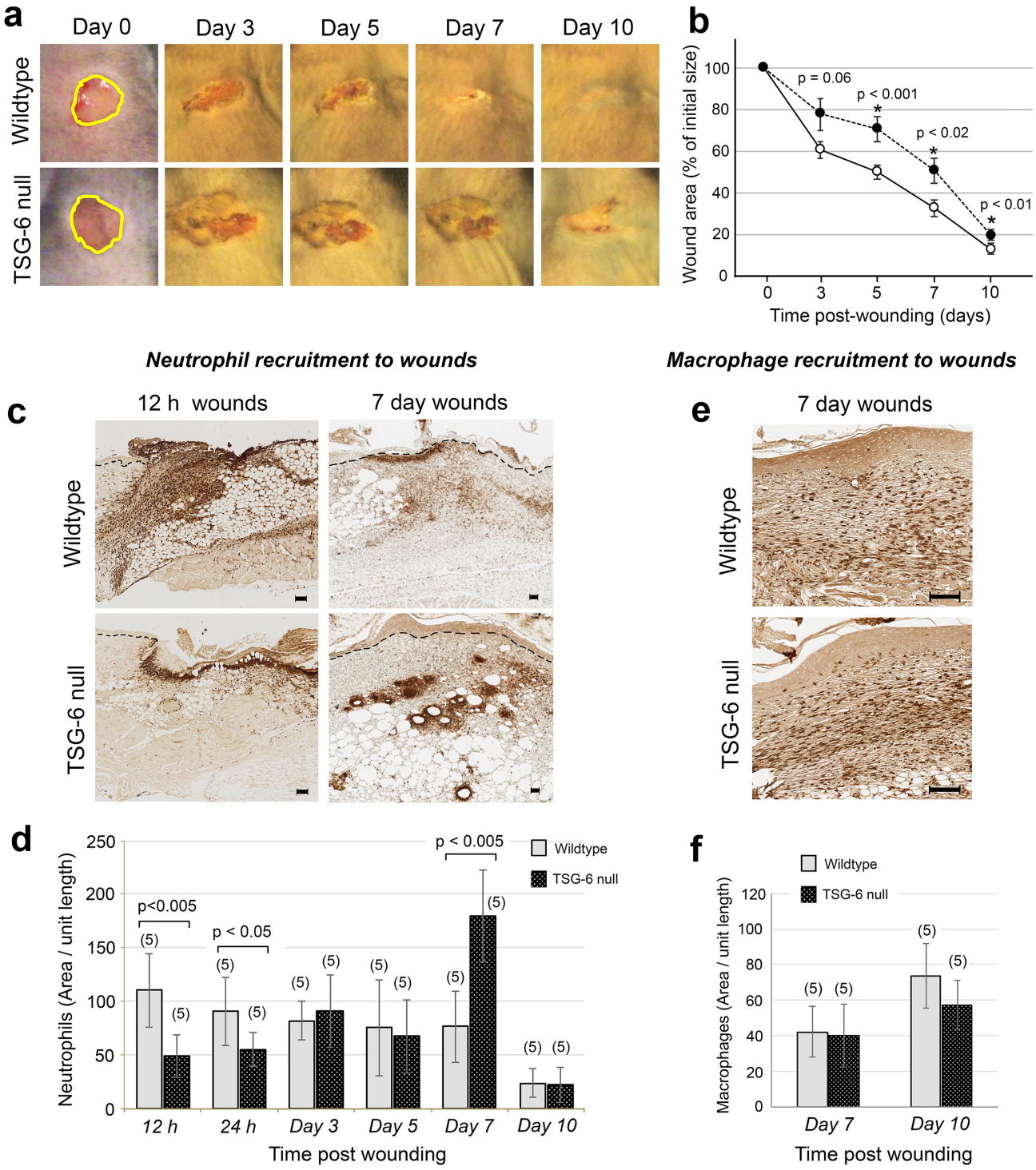
a
Day 0
Day 3
Day 5
Day 7
Day 10
Wildtype
TSG-6 null
b
Wound area (% of initial size)
p = 0.06
p < 0.001
p < 0.02
p < 0.01
Time post-wounding (days)
Neutrophil recruitment to wounds
Macrophage recruitment to wounds
c
12 h wounds
7 day wounds
Wildtype
TSG-6 null
e
7 day wounds
Wildtype
TSG-6 null
d
Neutrophils (Area / unit length)
p<0.005
p < 0.05
p < 0.005
Wildtype
TSG-6 null
12 h
24 h
Day 3
Day 5
Day 7
Day 10
Time post wounding
f
Macrophages (Area / unit length)
Wildtype
TSG-6 null
Day 7
Day 10
Time post wounding

Figure 3.

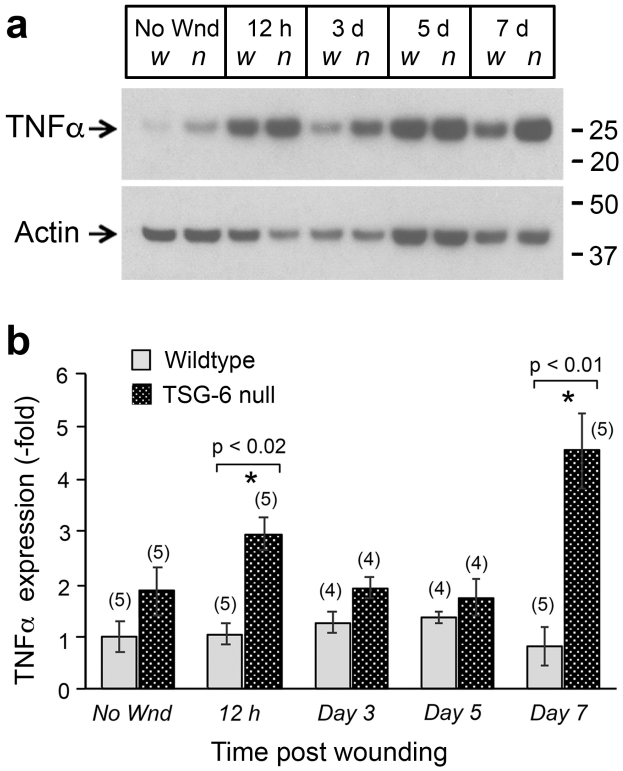
a
No Wnd
12 h
3 d
5 d
7 d
w n
TNFα
Actin
25
20
50
37
b
Wildtype
TSG-6 null
TNFα expression (-fold)
p < 0.02
p < 0.01
*
(5)
(4)
No Wnd
12 h
Day 3
Day 5
Day 7
Time post wounding

Figure 4.

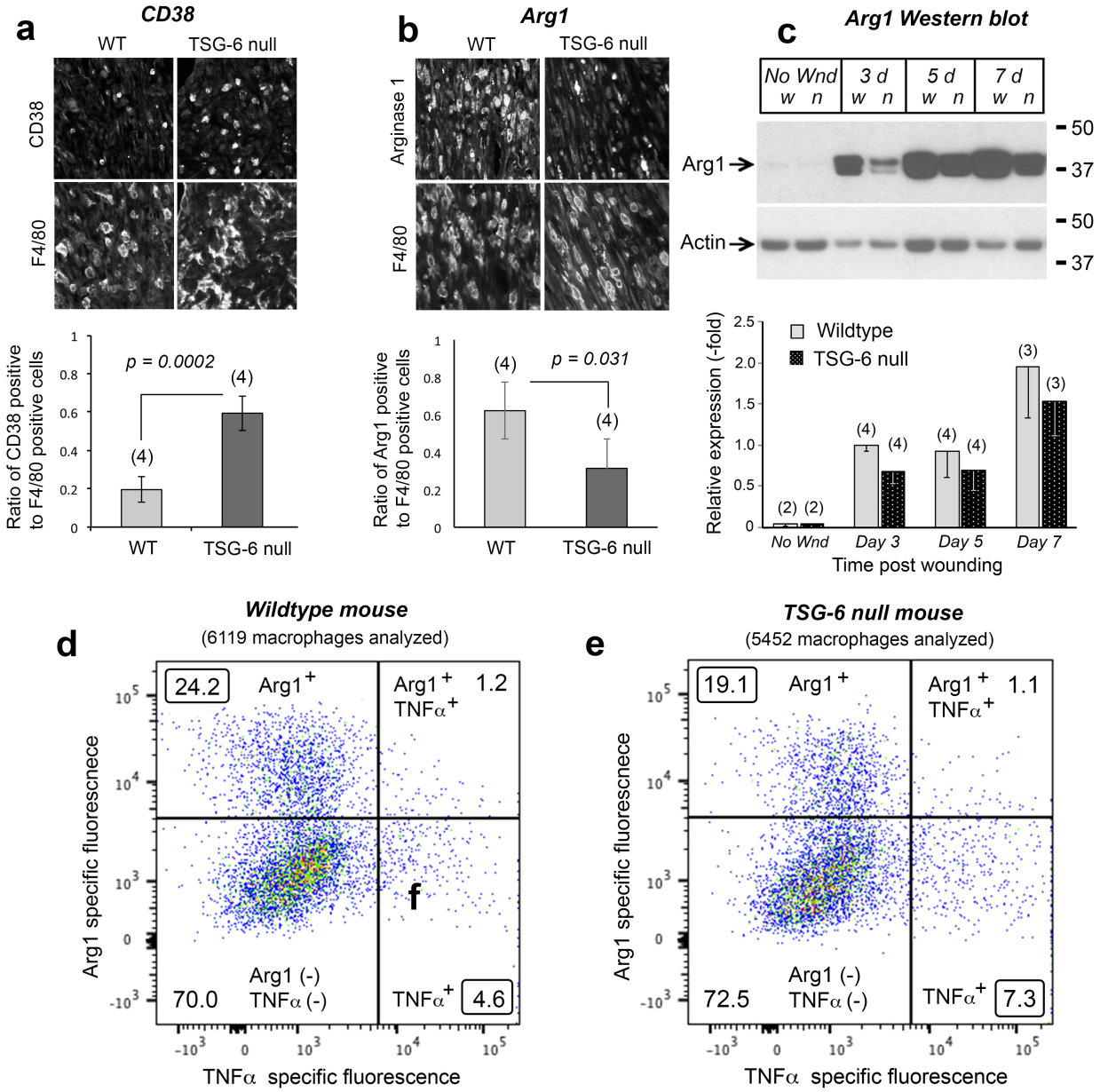
a
CD38
WT
TSG-6 null
CD38
F4/80
Ratio of CD38 positive to F4/80 positive cells
p = 0.0002
(4)
(4)
WT
TSG-6 null
b
Arg1
WT
TSG-6 null
Arginase 1
F4/80
Ratio of Arg1 positive to F4/80 positive cells
p = 0.031
(4)
(4)
WT
TSG-6 null
c
Arg1 Western blot
No Wnd
3 d
5 d
7 d
w n
Arg1
Actin
50
37
Relative expression (-fold)
Wildtype
TSG-6 null
No Wnd
Day 3
Day 5
Day 7
Time post wounding
d
Wildtype mouse
(6119 macrophages analyzed)
24.2
Arg1+
Arg1+ TNFα+
1.2
Arg1 (-) TNFα (-)
70.0
TNFα+
4.6
Arg1 specific fluorescnece
TNFα specific fluorescence
e
TSG-6 null mouse
(5452 macrophages analyzed)
19.1
Arg1+
Arg1+ TNFα+
1.1
Arg1 (-) TNFα (-)
72.5
TNFα+
7.3
Arg1 specific fluorescnece
TNFα specific fluorescence

Figure 5.

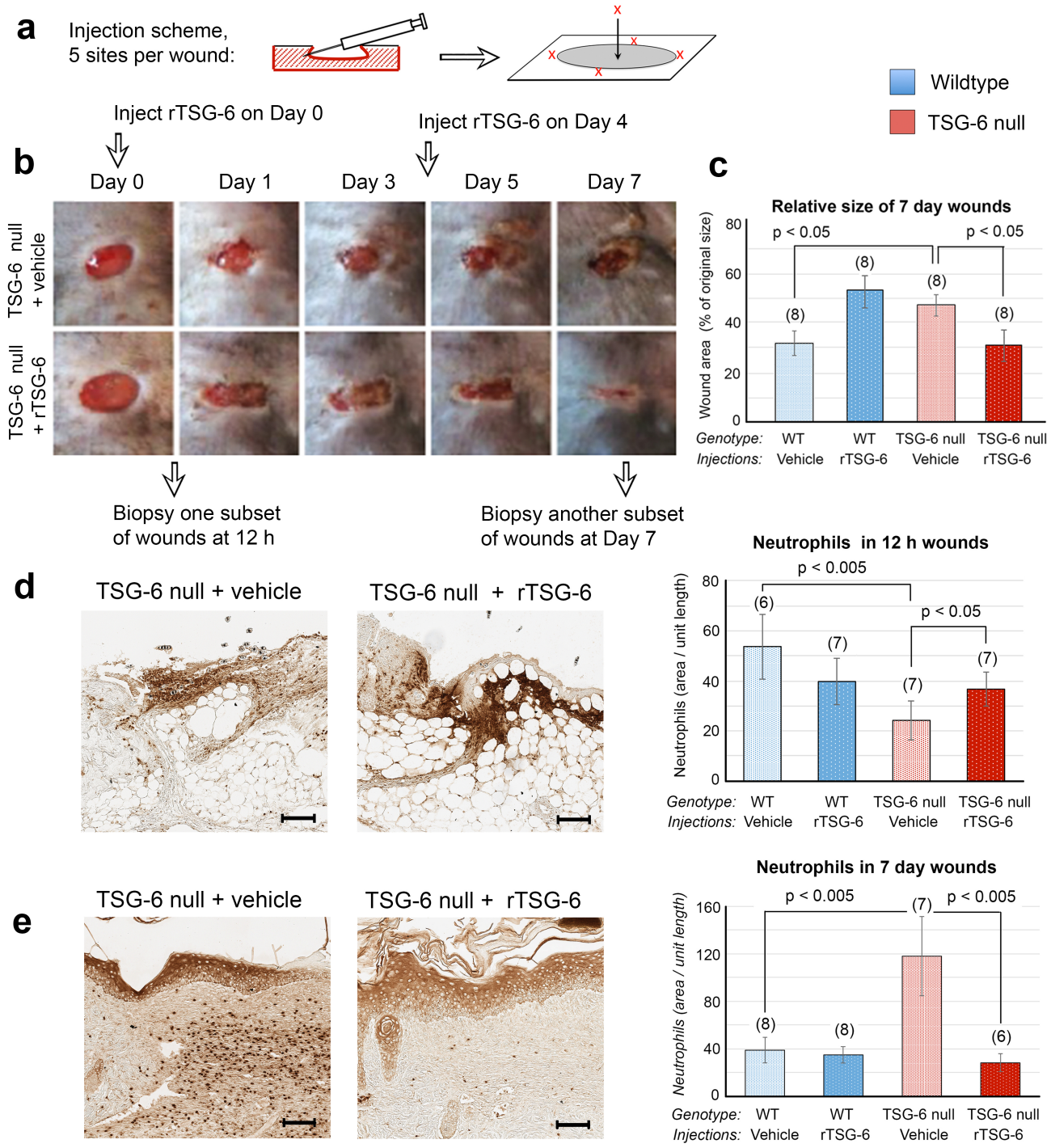
a
Injection scheme,
5 sites per wound:
Wildtype
TSG-6 null
Inject rTSG-6 on Day 0
Inject rTSG-6 on Day 4
b
Day 0
Day 1
Day 3
Day 5
Day 7
TSG-6 null + vehicle
TSG-6 null + rTSG-6
Biopsy one subset of wounds at 12 h
Biopsy another subset of wounds at Day 7
c
Relative size of 7 day wounds
Wound area (% of original size)
p < 0.05
p < 0.05
(8)
(8)
(8)
(8)
Genotype: WT WT TSG-6 null TSG-6 null
Injections: Vehicle rTSG-6 Vehicle rTSG-6
d
TSG-6 null + vehicle
TSG-6 null + rTSG-6
Neutrophils in 12 h wounds
Neutrophils (area / unit length)
p < 0.005
p < 0.05
(6)
(7)
(7)
(7)
Genotype: WT WT TSG-6 null TSG-6 null
Injections: Vehicle rTSG-6 Vehicle rTSG-6
e
TSG-6 null + vehicle
TSG-6 null + rTSG-6
Neutrophils in 7 day wounds
Neutrophils (area / unit length)
p < 0.005
p < 0.005
(8)
(8)
(7)
(6)
Genotype: WT WT TSG-6 null TSG-6 null
Injections: Vehicle rTSG-6 Vehicle rTSG-6